Study on influence of viaduct and noise barriers on the particulate matter dispersion in street canyons by CFD modeling

Chenrui Hao[a], Xiaomin Xie[a,*] xiexiaomin@sjtu.edu.cn, Yue Huang[b], Zhen Huang[a]

[a]Key Laboratory for Power Machinery and Engineering of M. O. E., Shanghai Jiao Tong University, No. 800, Dongchuan Road, 200240, Shanghai, PR China

[b]Institute for Transport Studies, University of Leeds, 34-40 University Road, Leeds, LS2 9JT, UK

*Corresponding author.

Abstract

This paper investigates the influence of viaduct, noise barrier, and the ratio of leeward and windward building height (H1/H2) on flow regime and particulate matters (PM) dispersion in an urban street canyon, using Computational Fluid Dynamic (CFD) simulation. Results show that viaduct introduces more sources of particulate and influences the flow pattern significantly. New vortexes form when noise barriers set up along the viaduct and influence the flow around the viaduct and distribution of pollutants at the center of the canyon but influence to a less extent in the key breathing zones. When the street canyon is symmetric, barriers can reduce the peak value of pollutant concentration at buildings wall, and lower the integral concentration in zones that affect people's breathing. When the street canyon is a step-up type (the leeward building is lower than the windward one), barriers affect to a less extent the PM distributions at buildings wall and breathing zones. Increase of the height of windward buildings hinders the diffusion of pollutants. Furthermore, people living in the windward building or walking on the street have to suffer more from the pollutant. When the street canyon is a step-down type (the leeward building is higher than the windward one), H1/H2 = 6/5, pollutants still gather at the leeward wall. It has the least integral pollutant concentration in the zone near buildings and street. H1/H2 = 2, pollutants are transported to the windward wall and accumulated because of the upper main vortex in the canyon. Pedestrians' breathing zone is extremely high compared with other configurations.

Keywords: Street canyon; Particulate matter; Viaduct; Noise barrier; CFD simulation

1 Introduction

With the increase in vehicle ownership and expansion of road networks in recent years, vehicle emission has become one of the main sources of PM (particulate matter (PM)). It is also listed as the pollutant most responsible for air quality deterioration in an urban environment (Scungio et al., 2018), even though the threshold values for light-duty (passenger and commercial) vehicles have been regulated based on the level of PM emissions (Commission, 2008). There is a relationship between exposure to these pollutants and getting lung cancer, although IARC (the International Agency for Research on Cancer) and WHO (World Health Organization) have classified airborne particles from outdoor air pollution as Group 1 carcinogens (Beelen et al., 2014a). What's more, it was recognized that long-term exposure to PM can also lead to cardiovascular disease (Beelen et al., 2014b; Wang et al., 2014).

Some types of urban street layout are known not good for pollutant's diffusion. One of the typical configurations that gathers pollutants most significantly and does harm to human is the so-called street canyon, which means a street flanked by continuous buildings on the two sides. Vortexes form due to buildings seated at both sides in this type of street layout. As the aspect ratios H/W (height of building, H; and width of the street, W) or the ratio of the leeward building and the windward building H1/H2 is the most influential feature of the street canyon, researches so far were focused on their influences (Li et al., 2005; Oke, 1988; Xiaomin et al., 2006). Besides the two ratios, other configurations of the buildings can also affect the wind regime and pollution dispersion (Kastner-Klein and Plate, 1999; Llaguno-Munitxa et al., 2017; Madalozzo et al., 2014; Ng and Chau, 2014). In fact, the thermal behaviors of buildings were also found to be influencing the pollutant dispersion (Allegrini et al., 2014; Sini et al., 1996; Tan et al., 2015; Xie et al., 2007).

Simulation of dispersion of gaseous pollutants is not the same as using a discrete phase model. Researchers have found that simulations between gaseous pollutant and particle showed different patterns in pollutant concentration (Carpentieri et al., 2011; Hang et al., 2016; Quang et al., 2012). That phenomenon is due to the process of particle dispersion including turbulent mixing and dilution, deposition and so on (Kumar et al., 2011). By investigating the dependence on wind characteristics, particle number distributions and concentrations, Hagler et al. (2012) and Kumar et al., (2008) -estimated the particle number flux and particle number emission factors in typical urban streets and driving conditions, by field measurements. Wind-tunnel experiments were carried out to study the particle dispersion and the influence by the building geometry such as height, roof shape or the surface temperature (Allegrini et al., 2013; Llaguno-Munitxa et al., 2017; Meroney et al., 1996; Nikolova et al., 2011). In addition to wind tunnel studies, 2D Computational Fluid Dynamic (CFD) studies were undertaken. For example, Santiago et al. (2008) established a 2D SLP- (street Lagrangian particles) model to calculate PM_{10} & $PM_{2.5}$ diffusion in street canyons, compared the results with measured values and found a good correlation. With the advancements in computing power, more 3D CFD simulations were used in recent researches (Bowker et al., 2007; He et al., 2017; Nikolova et al., 2011; Steffens et al., 2012). Jin et al. (2016) studied the spread of H_2SO_4 in a 3D model. Results showed that the wind direction is a key influence on the particle number concentration on leeward and windward walls. Furthermore, researchers investigated other aspects. Fallah-Shorshani et al. (2017) integrated a street-canyon model with a regional Gaussian dispersion model for improving the characterization of near-road air pollution. Zhong et al. (2017)'s study revealed the impacts of nonlinear O3-NOx-VOC photochemical processes in an incomplete mixing environment and provided a good description of the pre-processing of emissions within canyons, prior to their release to the urban boundary layer, by using a combination of street canyon dynamics and chemistry.

In more recent studies, the influence of other objects in the canyon such as plants and road barriers was also simulated (Moradpour et al., 2017; Neft et al., 2016; Wang et al., 2017; Wania et al., 2012). With the growth of cities and road networks, more and more viaducts are built over main roads. Viaducts have become a common structure in international metropolises. The existence of a viaduct in the canyon can influence the dispersion of pollutants. On one hand, viaduct facilitates the movement of more vehicles into the canyon, which increases the emission sources. On the other hand, it can change the flow pattern, which can influence the pollutant concentration pattern. Noise barriers are built to reduce the impact of traffic noise on residents. Meanwhile, they can also influence the pollutant dispersion by influencing the flow pattern. Unfortunately, there are few literatures concerning this typical layout of street canyons using a real size simulation. Baldauf et al. (2016) measured the pollutant dispersion near a large highway in Phoenix, Arizona, USA to study the influence of noise barriers on air quality. Venkatram et al. (2016) developed an 1D model to simulate to impact of noise barriers on near road air quality and showed good agreements with Baldauf et al.'s measurements (Baldauf et al., 2016). Studies above showed that barriers have great impact on pollutant dispersion. Hang et al. studied the flow and CO dispersion in a symmetric canyon with H/W = 1 or 0.5 (Hang et al., 2017), and analyzed the effects of viaduct, road barriers and ground heating on gaseous pollutant dispersion and particle distribution in a symmetric canyon with H/W = 1 (Hang et al., 2016). It was found that the viaducts reduced the overall indoor pollutant concentrations because they slowed down the flow above viaduct and strengthened particle deposition onto the viaduct surface. He et al. (2017) simulated the flow and CO dispersion in deep canyons with H/W ratio from 1 to 5. From these articles, conclusions were drawn that viaducts and noise barriers have large impacts on pollutant dispersions and there are still more things remained to study with this canyon structure. These researches paid more attention to gaseous pollutant and the canyons are ideal street canyons that aspect ratio H/W is greater or equal to 1, the buildings alongside are with equal height. However, typical street canyons with viaducts and barriers always have low H/W ratio and the buildings alongside are seldom symmetric. Previous researches indicated that street canyon configuration is one of the most important factors that affect the characteristics of flow regime and pollutant dispersion in the street canyon (Madalozzo et al., 2014; Oke, 1988; Xie et al., 2006). Therefore, there should be more researches concerning PM dispersion in street canyons close to the real environment. This paper develops a dispersion model based on discrete phase model (DPM). In order to study the characteristics of PM dispersion in street canyon with complicated configurations that include viaducts, noise barriers, and asymmetrical buildings, three types of street canyons are discussed: symmetric canyons, step-up canyons and step-down canyons. Viaducts and noise barriers in these three types of canyons are studied, to evaluate the influence of viaducts and noise barriers on the flow and PM dispersion patterns. Findings from this study shall by interested by environmental scientists and transport planners who aim to model and reduce air pollution levels in the urban traffic environment.

The structure of the paper is as follows. Section 2 describes the model structure, flow and dispersion modeling setups in CFD simulations. Section 3 presents CFD validation by experimental data. Results are discussed in Section 4, and Section 5 draws the conclusion and reflects on the research approach.

2 Numerical simulation

2.1 Site description

According to Shanghai Master Plan for 2017–2035, there will be 320 km viaducts built in this city, accounting for 25% of the total main road length ~~(Shanghai Government, 2018)~~[Instruction: Insert (Shanghai Government, 2018)]. The contribution of mobile emission sources to the concentration of PM in Shanghai ranks fourth in China's cities. (China Vehicle Environmental Management Annual Report, 2018). Therefore, Shanghai is considered as a typical case in this study in order to make the research more impactful. North Zhongshan Road is an ideal street canyon as there is a viaduct Inner Ring Elevated Road. It is located at 31°14′34.5″N and 121°25′17.8″E. A map of the location within this area is given in Fig. SM1.

The street is about 60 m wide with 8 traffic lanes which take 40 m in total. The viaduct is 10 m high and has six lanes. The thickness of the viaduct is 2 m. The distance between the two bridge piers is about 20 m, much larger than the thickness of a pier. Therefore, piers are not included in the model. The street-side buildings are residential buildings and 20 m tall. A 2D model can be developed as drawn in Fig. 1. In this model, the aspect ratio is 1/3, which means that it is a wide canyon. Besides, along North Zhongshan Road, there are other street canyons that have different buildings on the two sides, one is the same residential building as described above; the other is a 24 m tall hotel and a 40 m tall office building. Table 1 lists the configurations studied in this paper.

Fig. 1

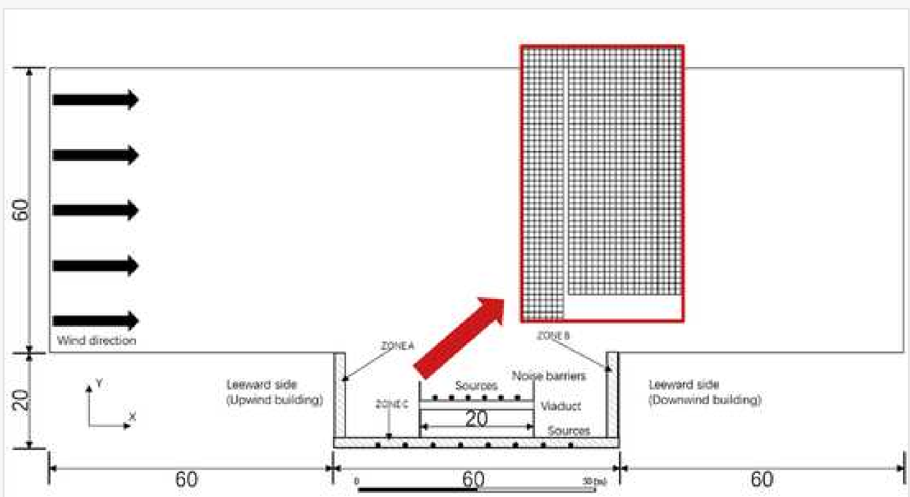

Configuration, observation zones of the street canyon and grid detail in CFD simulation around the noise barrier.

alt-text: Table 1

Table 1

The presentation of Tables and the formatting of text in the online proof do not match the final output, though the data is the same. To preview the actual presentation, view the Proof.

Summa[Instruction: TW: In the proof, this table is not shown perfect. But i cannot edit it in the proof. Could you please adjust the column width to make it more perfect?]ry of configurations in the CFD model.

Canyon Type	Case Name	Viaduct & Barrier	Leeward Height	Windward Height	H1/H2	H/W
Symmetric canyon	NV	Without viaduct	20	20	1/1	1/3
	VO1/1	With viaduct	20	20	1/1	
	VB1/1	With viaduct & barrier	20	20	1/1	
Step-up canyon	VO1/2	With viaduct	20	40	1/2	
	VB1/2	With viaduct & barrier	20	40	1/2	
	VO5/6	With viaduct	20	24	5/6	
	VB5/6	With viaduct & barrier	20	24	5/6	
Step-down canyon	VO2/1	With viaduct	40	20	2/1	
	VB2/1	With viaduct & barrier	40	20	2/1	
	VO6/5	With viaduct	24	20	6/5	
	VB6/5	With viaduct & barrier	24	20	6/5	

The dispersion of pollutants varies depending on the flow patterns caused by the different canyon configurations. Therefore, all the factors considered in this paper have an influence on human health. In order to make it more intuitive, three key zones that influence human health mostly are set to study the integral pollutant concentration (Fig. 1). Zone A and zone B are set close to the leeward building and windward building respectively with 2 m width. These two zones influence people live or work in the building. Zone C is set one the ground with a 2 m height. Pollutant in zone C harms the health of the pedestrian.

Here, H1 stands for the leeward building, H2 stands for the leeward building. As for case names, NV stands for ‘no viaduct’, VO for ‘viaduct only’ and VB for ‘viaduct with barriers’. The number at the end means represents the H1/H2 ratio.

2.2 CFD setups in flow modeling

Computational fluid dynamics modeling is based on numerical solutions to the dispersion equation and the simulation of fluid flow, which are derived from the conservation and transmission principles. The air within the street canyon can be considered an incompressible turbulent inert flow, and the air and pollutant density is assumed constant. As stated by Sini et al. (1996), these assumptions are reasonable for most low-level atmospheric environments. In addition, turbulence due to buoyancy effects is not taken into consideration, as thermal effects in street canyons are not included in this study.

Three types of steady RANS turbulence models (standard, RNG, Realized $k-\varepsilon$ method) were filtered by comparing with wind-tunnel experiment (Allegrini et al., 2014) in this study. The conservation equations are attached in Supporting Materials. According to Yoshie (2007)'s research, steady RANS turbulence models have limitations in predicting turbulence. For example, they cannot predict the length of reattachment behind buildings and they underestimate the speed of weak wind regions. Despite the limitations, steady RANS turbulence models have been widely applied because they are successfully validated in predicting average airflows (Hang et al., 2016) and flow around building (Ai and Mak, 2017). Many researchers have applied the steady RANS turbulence models in their studies, such as the RNG $k-\varepsilon$ method (Habilomatis and Chaloulakou, 2015; Li et al., 2016; Xie et al., 2006), the Standard $k-\varepsilon$ method (Kim and Baik, 2001; Kumar et al., 2009; Xiaomin et al., 2006) and Realizable $k-\varepsilon$ method (Allegrini et al., 2014; Moonen et al., 2011; Moradpour et al., 2017).

The commercial CFD software Fluent (2009) is used to implement the mathematical model above. In addition, the governing equations are discretized using the finite volume method and the second-order upwind scheme. The SIMPLE scheme is used for the pressure and velocity coupling.

The inlet flow velocity is expressed in an exponential f[Instruction: OT: The equation is correct. But in the proof, all the equations (Eq.1-3) are splited in different lines by the equal signs. Please check it.]unction:

$$u(z) = U_0\left(\frac{z-H}{Z}\right)^{\alpha} \tag{1}$$

where U_0 is the a common wind speed in Shanghai which is 3 m/s (Gu et al., 1997; Li et al., 2007). H is the height of the building and Z is the thickness of the boundary layer which is 80 m in the paper. This thickness is also applied in Ai and Mak's simulation (2017). α is set to 0.22 which is the wind profile exponent indicating the base surface roughness in relation to the terrain category of the mid-dense urban area (Hang et al., 2017). The outlet is set with outflow condition. The top domain is set as symmetrical. The other walls include buildings, viaduct, noise barriers; and the bottom street are all defined as non-slip walls with standard wall function.

Fig. 1 also shows the mesh details in the model in the expanded box. As the thickness of the noise barrier has been set to 0.1 m, the minimum size cannot be larger than 0.1 m. Smaller size will prolong the computational time but have little influence on the results. So the minimum grids are set as 0.1 m * 0.1 m. Grids of this size are applied to the whole area inside the canyon. However, the grids above the canyon and buildings become bigger as they have little effects. The convergence criteria of all residuals is set to 1e-6.

2.3 CFD setups in dispersion modeling

In order to simulate the inert PM dispersion, a discrete phase model (DPM) in ANSYS Fluent is used (Fluent, 2009). The trajectory of a discrete phase particle (or droplet or bubble) is predicted by analyzing the forces on the particle, which is written in a Lagrangian reference frame. This force equation includes the particle inertia and the forces acting on the particle, and can be written as:

$$m_p\frac{d\vec{u}_p}{dt} = m_p\frac{\vec{u}-\vec{u}_p}{\tau_r} + m_p\frac{\vec{g}\left(\rho_p-\rho\right)}{\rho_p} + \vec{F} \tag{2}$$

where m_p is the particle mass, $\vec{u}$ is the fluid phase velocity, $\vec{u}_p$ is the particle velocity, ρ is the fluid density, ρ_p is the particle density, $\vec{F}$ is an additional force, $m_p \frac{\vec{u}-\vec{u}_p}{\tau_r}$ is the drag force, and τ_r is the droplet or particle relaxation time (Gosman and Ioannides, 1983) calculated by:

$$\tau_r = \frac{\rho_p d_p^2}{18\mu} \frac{24}{C_d \mathrm{Re}} \quad (3)$$

here, μ is the molecular viscosity of the fluid, d_p is the particle diameter.

An eight-point group source on the ground is used to simulate the eight-line street, and six-point group source on the viaduct to simulate the six-line viaduct (Fig. 1). The initial speeds of the particles are all set to zero. The Rosin-Rammler Diameter Distribution Method is used to set the diameter of the particles. The mean diameter used in this study referred to Li et al. (2007)'s work.

3 CFD validation

3.1 CFD validation of flow modeling

It is known that model validation is a vital step in CFD modeling before actual simulations. Therefore, a 2D isolated canyon model was built in order to evaluate the accuracy of the turbulent model of this study. Allegrini et al. (2014) constructed a wind tunnel made of aluminum plate to measure the flows in street canyon, then did a series of two-dimensional CFD simulations using different wall functions and compared the results with his wind-tunnel measurement. Validation results in this paper were compared with the wind-tunnel experiments from Allegrini et al. (2014). Canyon for validation was built in accordance with Allegrini et al. (2014)'s approach as well. In this case, the model was 0.855 m high and 8.880 m long. The distance between the canyon and the inlet domain is 7.4 m and outlet domain 1.2 m. The canyon is 0.2 m wide while its aspect ratio is 1. The geometry and grids can be seen in Fig. SM2. Different minimum cell sizes are tested to verify the grid independence. The results are shown in Fig. 2(a). When minimum cell size is 0.002 m or 0.001 m, results show good agreements with Allegrini et al. (2014)'s measurement. Since the smaller cell size costs much more computation time, the grid size inside the canyon used in the validation was $\Delta x = \Delta y = 0.002m$. The total grid number was 26,954. The convergence criteria of all residuals is set to 1e-6. The 3 different types of $k-\varepsilon$ model (standard, RNG, Realized) were all tested to verify the best model that match the experiment result. Furthermore, in order to study the effect of wall functions on the results, Low Reynolds Number Method (LRNM) and 3 types of near-wall treatments including Standard Wall Function (SWF), Scalable Wall Function (SCAWF) and Enhanced Wall Treatment (EWT) were applied in validation. Their results of normalized vertical velocity (V/U) were compared with Allegrini et al. (2014)'s data to draw a conclusion.

Fig. 2

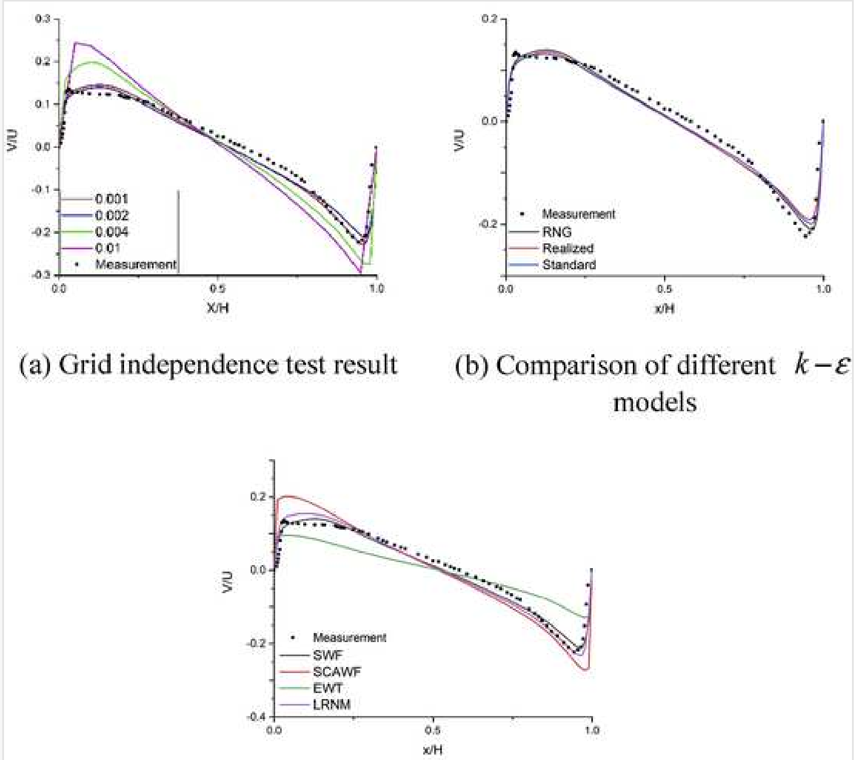

(a) Grid independence test result

(b) Comparison of different $k-\varepsilon$ models

(c) Comparison of different near-wall treatments

Flow validation from CFD simulations and wind-tunnel data on normalized vertical velocity.

Fig. 2(b) and (c) show the normalized vertical velocity (V/U) at half canyon height (y=0.5H). All the simulation results show high similarity with experiments by Allegrini et al. (2014). It can be seen clearly that the results for velocity using the SWF function are the most accurate. Thus, the SWF function is applied. On the other hand, there is little difference between the outputs of different $k-\varepsilon$ models. Considering its wide application and good performance. As a result, the RNG $k-\varepsilon$ model using SWFs as near-wall treatment is used in this study.

3.2 CFD validation of pollutant dispersion modeling

The pollutant dispersion model in this paper was compared with another wind-tunnel test by Meroney et al. (1996). Fig. 3(a) shows the measurement points. The RNG $k-\varepsilon$ turbulence model with SWF was used here for reasons stated in Section 3.1. All the other settings were the same as in Section 3.1. The pollutant source is set in the center of the canyon ground. And setups of particle diameter is the same as the one discussed in Section 2.3. In order to compare experimental results and calculated results more easily, the concentration of each measurement point is expressed as a ratio to the highest concentration point. The highest concentration point is P7. Thus the normalized concentration is calculated by C/C_7. A similar data processing method was used by Xia and Leung (2001). The comparison results are depicted in Fig. 3(b). Overall, values from the simulation result are close to the experimental data. The computed result at the sixth point is lower than the wind-tunnel result. The small errors may be caused by different canyon structure. Meroney et al. (1996) used a non-isolated canyon in their study while the canyon in this paper is an isolated one. It is in good correlation with the experimental data except for the sixth point. Besides, a linear regression and three statistical parameters (normalized mean square error, NMSE and correlation R) were calculated to compare the two results for more detailed evaluation. As R=0.989, NMSE=0.171, this indicated a high-quality simulation. The linear regression curve is shown in Fig. 3(c). Therefore, these model setups can be accepted. The following section will discuss the simulation results using this model in a real scale street canyon.

Fig. 3

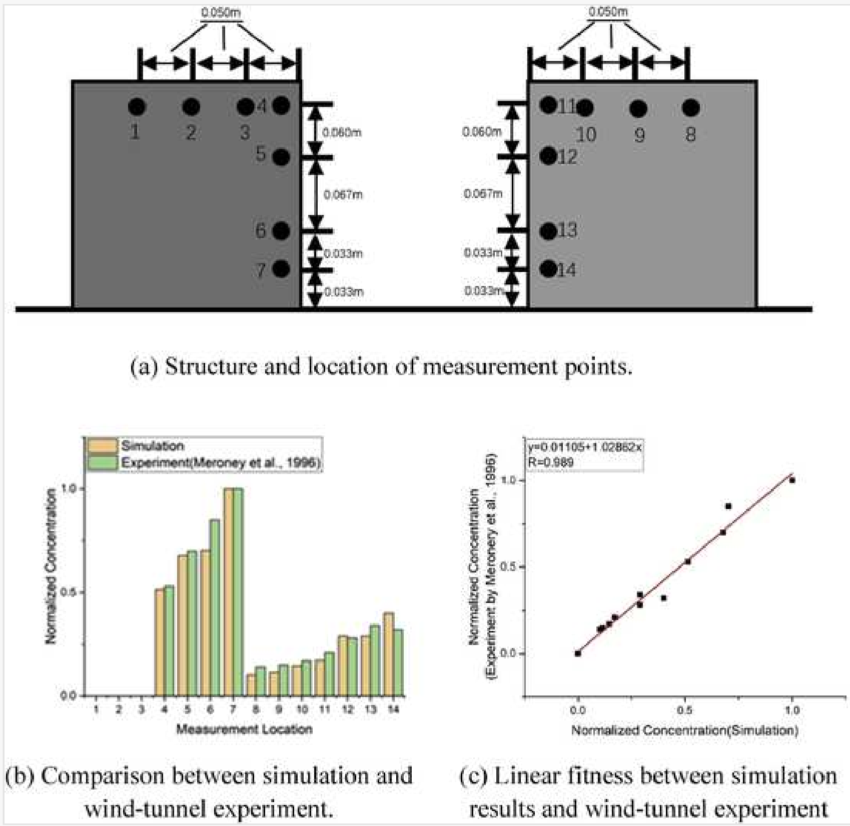

Dispersion validation from CFD simulations and wind-tunnel data.

4 Results and discussion

In order to get a more universal conclusion, configurations investigated in this paper are divided into three groups: symmetric street canyons (H1/H2=1), step-up street canyons (H1/H2<1) and step-down street canyons (H1/H2>1).

4.1 Flow pattern and dispersion pattern in a symmetric street canyon

Effect of a viaduct and noise barriers in a symmetric street canyon is presented in this section. The flow and dispersion patterns are shown in Fig. 4. As shown in Fig. 4(a), a main vortex forms in the canyon and its center is located near the windward wall. As a result, flow streams are more intensive near the windward side. Due to the vortex being clockwise, a higher concentration of pollutants is on the leeward side (Fig. 4(b)).

Fig. 4

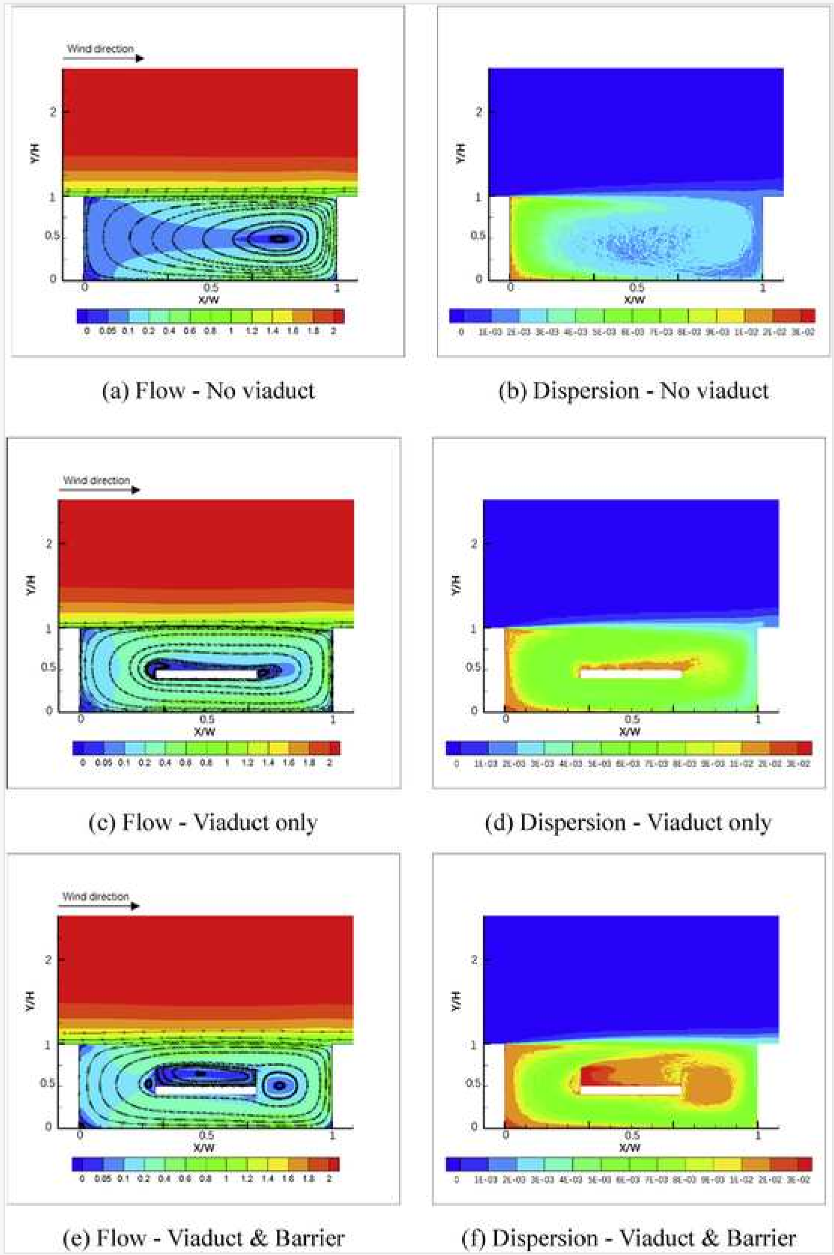

Flow pattern and dispersion pattern in a symmetric street canyon.

When there is a viaduct (Fig. 4(c)), the vortex is divided into two weak ones and distributed on both sides of the viaduct. When there is a viaduct in the canyon, more sources of particulate are introduced (Fig. 1). As a result, the DPM concentration in the canyon enhances (Fig. 4(d)). The pollutants released from the vehicles in the viaduct are taken to the canyon by the wind. It can be seen that there is a higher concentration of pollutants on the leeward side. Few pollutants remain on the windward side of the viaduct due to the weak secondary vortex at the windward side.

Three clockwise vortexes form when there are noise barriers on the viaduct (Fig. 4(e)). There are two main vortexes, one is above the viaduct while the other at the right-hand side of the viaduct. As a result, the flow speed above the viaduct gets lower. The presence of noise barriers mainly changes the flow around the viaduct.

Some pollutant is stuck inside the viaduct canyon and gathers along the leeward side of the viaduct when the noise barriers are located (Fig. 4(f)). More pollutants than in Fig. 4(d) gather near the windward side close to the windward noise barrier. That phenomenon is related to the stronger vortex at the windward side of the street canyon.

Vertical profiles of concentration at the windward wall and leeward wall are shown in Fig. 5(a) and (b). Fig. 5(a) shows a peak between 1.5 m and 2 m at the windward wall. This level of concentration poses harmful health effects to pedestrians on the sidewalk near the windward wall. This phenomenon is especially obvious in the VO1/1 configuration and its peak is coincidentally found at 1.5 m height which is about the height of the breathing zone of adults. At height over 2.2 m, VO1/1 and VB1/1 show little difference in the concentration which is still higher than the NV1/1 configuration. This is easy to understand because there are more pollutant sources in case VO1/1 and VB1/1. Fig. 5(b) shows vertical profiles of concentration at the leeward wall. When a viaduct is added to the street canyon, the leeward wall concentration is higher at almost all heights. However, VO1/1 configuration has the highest concentration level at heights over 15 m but the concentration below 10 m is comparable with NV1/1 configuration. That means viaduct mainly increase the pollutant concentrations at the height over 15 m at the leeward wall. Under an assumption that each floor is 3 m high, the affected floors are from the fourth floor to the sixth floor in this case. Viaduct with noise barriers increases the concentration level compared with no viaduct. At heights above 15 m, the difference is more profound. Fig. 5(c) shows the horizontal profiles of concentration at the height of the breathing zone (1.5 m). At this height, pollutant concentration near the leeward side is much higher than in the windward side, across all three configurations. It is clear to see that noise barriers on viaduct increase the concentration in the canyon at a height of 1.5 m.

Fig. 5

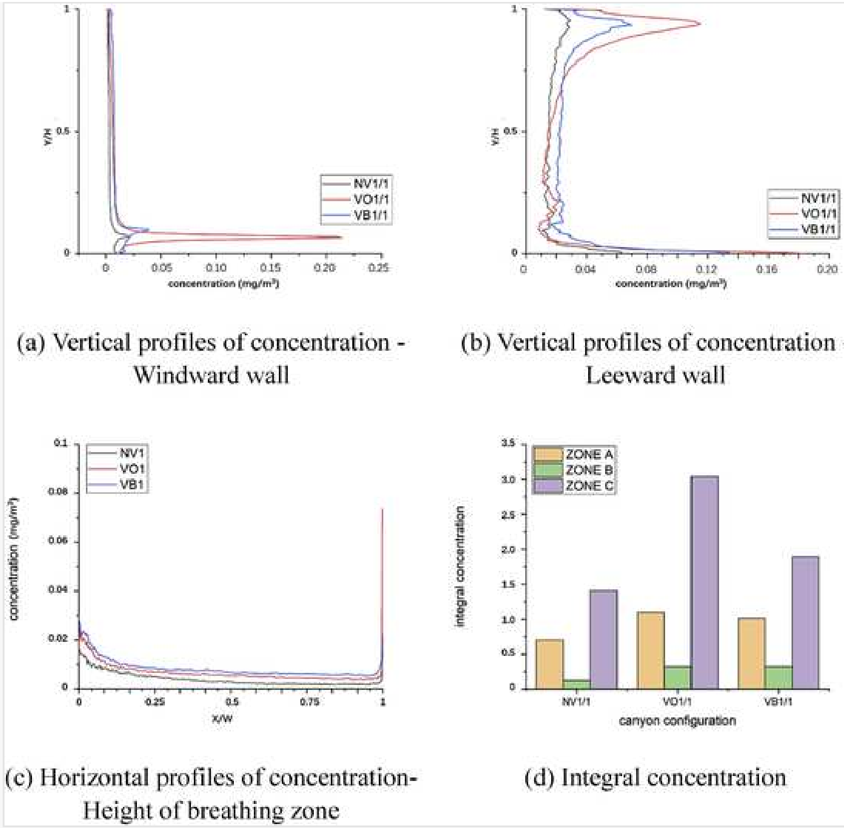

Concentration in symmetrical street canyons.

More detailed information can be obtained from the integral concentration comparison (Fig. 5(d)). Zone B represents the lowest integral pollutant concentration. The integral concentration of zone A is nearly 6 times higher than zone B. However, it is the pedestrians who suffer most as zone C's integral concentration is much higher than the other two. When a viaduct is built, pollutants in zone C increased by more than two times compared with NV1/1 situation. Meanwhile, integral concentration in zone B is three times more than in Case NV1/1, while zone A is nearly two times more than in Case NV1/1. After noise barriers are used, integral concentration in zone A-C has been reduced in varying degrees. Among them, the integral concentration of zone C has the most significant decrease. In conclusion, because of more pollutant being introduced when there is a viaduct, more harmful effect is to people inside the canyon. Furthermore, people work or live in buildings on the leeward side are mostly affected. Noise barrier can help to reduce the integral concentration in the areas that affect people's breathing. Pedestrians exposed on the street breath in less pollution and benefit most from this structure. Therefore, noise barriers can reduce the health impacts of vehicle emission on people in this type of street canyons.

4.2 Flow pattern and dispersion pattern in a step-up street canyon

Fig. 6 (a)-(h) show the effect of a viaduct with or without noise barrier while the leeward building is lower than windward. Similar to the flow pattern of Case NV1/1, there are two vortexes when there are no noise barriers on the viaduct in an H1/H2 = 5/6 canyon (Fig. 6(a)). But compared to Fig. 4(c), both vortexes get stronger and the centers of them move up when H1/H2 = 5/6. Due to the flow, most pollutants released by the viaduct gather near the two side of the viaduct (Fig. 6(b)), which is also the vortex center. In addition, pollutants released from the street are carried to the leeward of the canyon.

Fig. 6

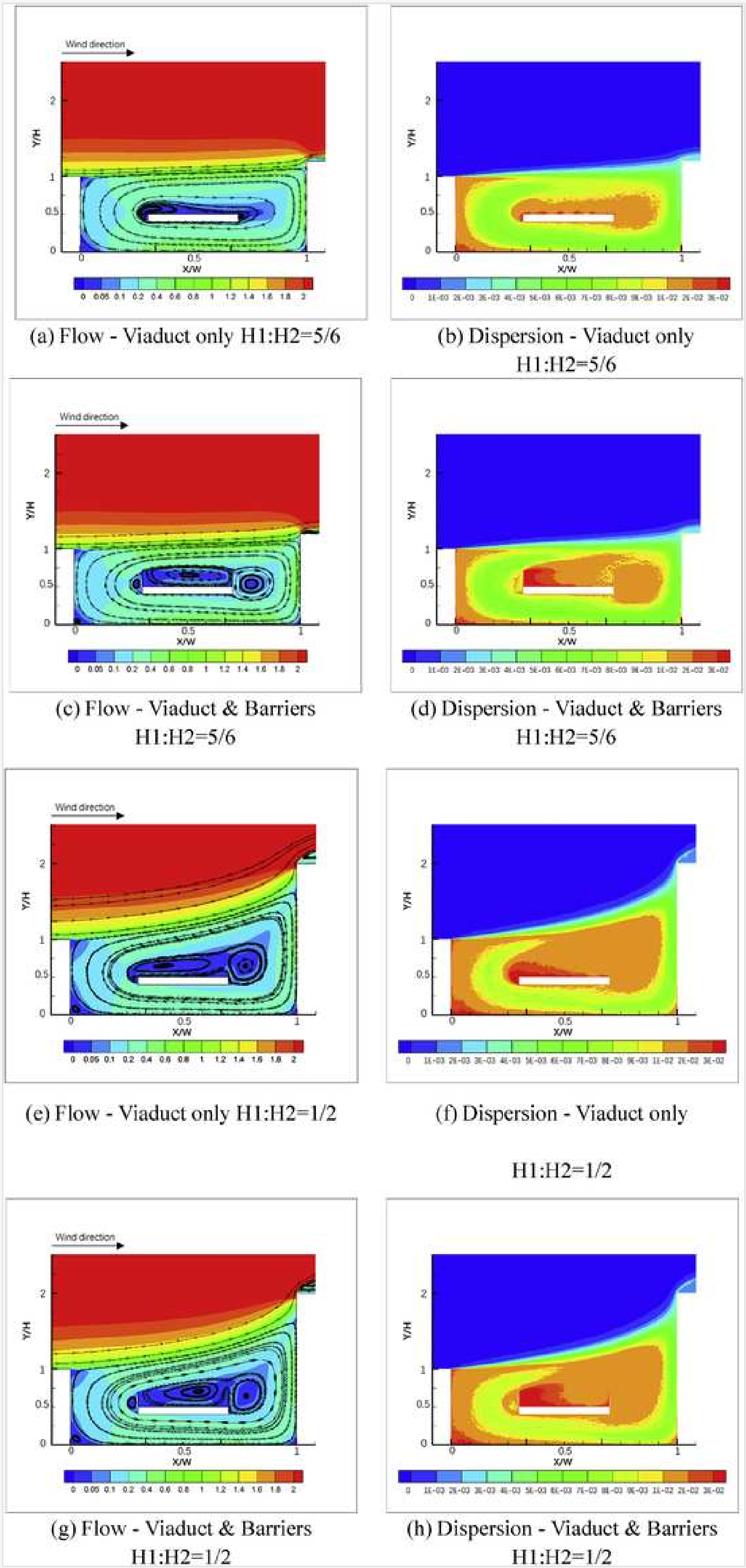

(a) Flow - Viaduct only H1:H2=5/6

(b) Dispersion - Viaduct only H1:H2=5/6

(c) Flow - Viaduct & Barriers H1:H2=5/6

(d) Dispersion - Viaduct & Barriers H1:H2=5/6

(e) Flow - Viaduct only H1:H2=1/2

(f) Dispersion - Viaduct only H1:H2=1/2

(g) Flow - Viaduct & Barriers H1:H2=1/2

(h) Dispersion - Viaduct & Barriers H1:H2=1/2

Flow pattern and dispersion pattern in a step-up street canyon.

When noise barriers are added in this canyon (Fig. 6(c)), vortexes are divided into three, including two strong ones and a weak one which shows a similar phenomenon with Fig. 4(e). The presence of noise barriers also weakens the flow above the viaduct but has little effect on the rest of the area. Some pollutants are trapped inside the canyon and gather at the leeward side of the viaduct when the noise barriers are located (Fig. 6(d)). Particles gathered near the windward side close to the windward noise barrier is bigger than in Fig. 6(b). This phenomenon is related to the stronger vortex at the windward side of the street canyon.

When H1/H2 = 1/2 (Fig. 6(e)–(h)), the vortexes further develop and move up. The left vortex climbs up to the upper surface of the viaduct in Case VO1/2 (Fig. 6(e)). Noise barriers sever the left vortex into two, one above the viaduct and the other on the left-hand side of the leeward barrier (Fig. 6(g)). Due to the flow, most pollutants released by the viaduct gather at the upper left edge of the viaduct (Fig. 6(f)) and are transported towards the upper right. Pollutants released from the street are carried to the leeward of the canyon. Noise barriers in this type of street canyon gather the pollutants released from viaduct inside the canyon (Fig. 6(h)). However, the pollutants are still taken to the upper right above the viaduct by the main vortex. The influence of noise barriers When H1/H2 = 1/2 on pollutant dispersion is not so big as when H1/H2 = 5/6. This is because vortexes have already formed above the viaduct when there are no barriers.

Fig. 7(a) shows the vertical profile of concentration at the windward wall. It can be seen that in a windward building, the higher people live or work, the fewer pollutants they are exposed to. At the windward wall, the peak points appear at about the same height (2 m above the ground) in all four configurations and the peak values are similar. Apart from the peak point, the concentrations of Case VO1/2 and VB1/2 are higher than Case VO5/6 and VB5/6 at the same heights. Moreover, noise barriers do not affect the vertical profile of concentration at the windward wall. Fig. 7(b) shows the vertical profile of concentration at the leeward wall. It can be seen that in a leeward building, the higher people live or work, the more pollutants they are exposed to. At the leeward wall, the peak points appear at about 19 m above the ground in all four configurations. But near roof level, there is a double peak in VO cases but a single peak in VB cases. Meanwhile, noise barriers enhance the peak value no matter near roof level or near ground level. Apart from the peak point, the concentrations of Case VO1/2 & VB1/2 are higher than Case VO5/6 & VB5/6 at most height, and noise barriers do not affect the vertical profile of concentration at the leeward wall. Fig. 7(c) shows the horizontal profiles of concentration at height of the breathing zone (1.5 m). It is clear to see that the increase of H1/H2 ratio leads to the decrease of concentration at the height of breathing zone and barriers do not affect the particle concentration. Meanwhile, concentration near the leeward side is significantly higher than the windward side. The following conclusions can be drawn from Fig. 7(d) by comparing the overall concentrations within the canyon. Firstly, noise barriers do not affect the pollutant concentration in zones that affect people's breathing. Secondly, the decrease of H1/H2 ratio leads to the increase of concentration in zones that affect people's breathing. Thirdly, pedestrians walking near the leeward side are exposed to more pollution than near the windward side.

Fig. 7

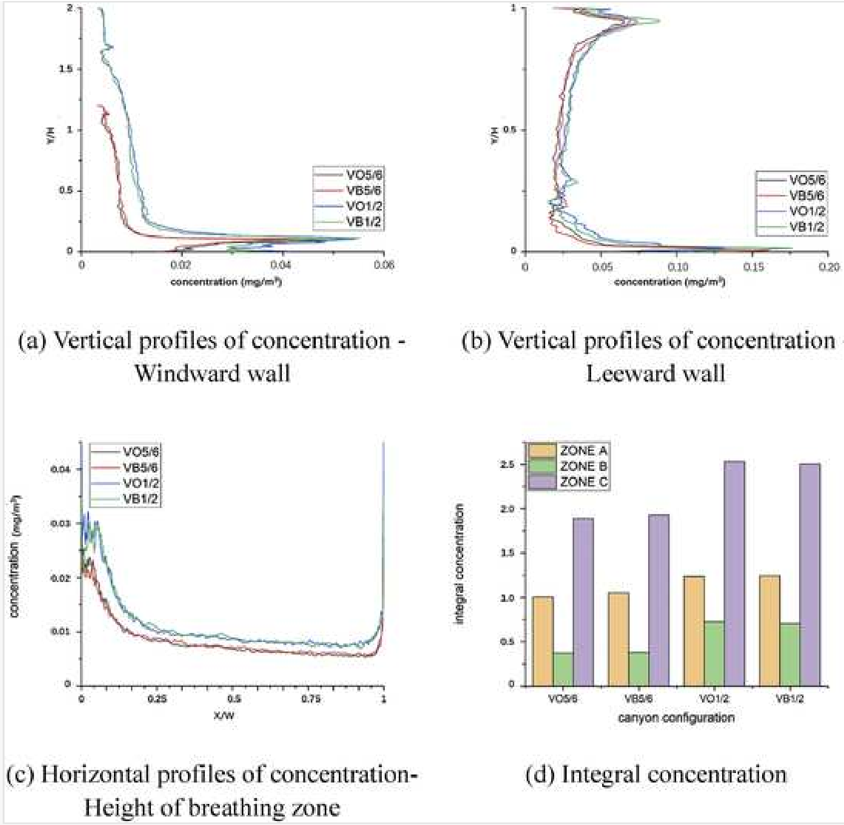

(a) Vertical profiles of concentration - Windward wall

(b) Vertical profiles of concentration - Leeward wall

(c) Horizontal profiles of concentration- Height of breathing zone

(d) Integral concentration

Concentration in a step-up street canyon.

4.3 Flow pattern and dispersion pattern in a step-down street canyon

Fig. 8 (a)-(h) shows the comparison between a viaduct with or without noise barrier when the leeward building is higher than windward. Different from other VO cases, there is only one vortex near the leeward in Case VO6/5 (Fig. 8(a)). In this case, pollutants mainly locate near the viaduct and at the leeward side of the canyon (Fig. 8(b)). However, the diffusion effect is stronger because the vortex is much stronger and has a higher velocity.

Fig. 8

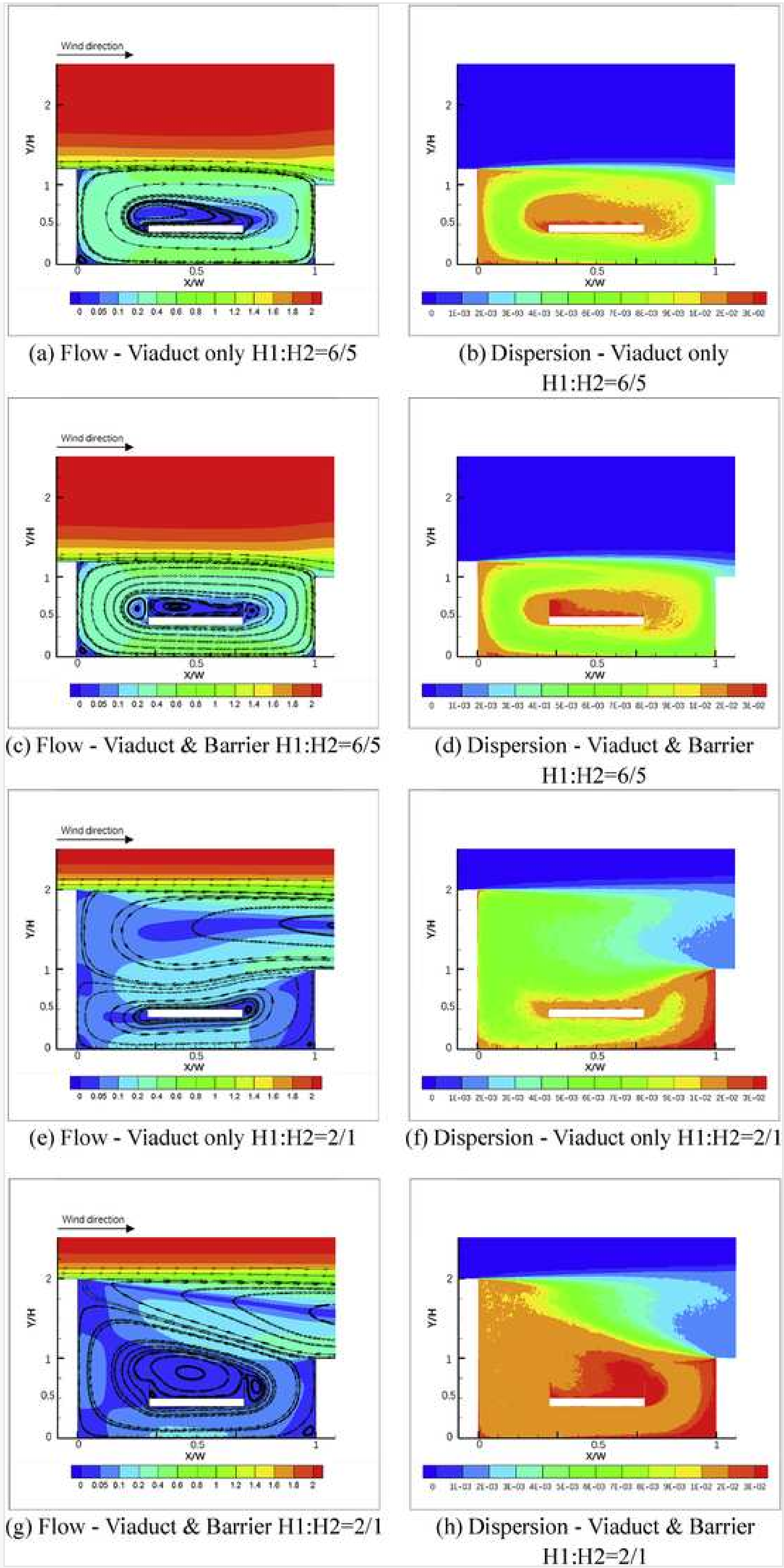

(a) Flow - Viaduct only H1:H2=6/5

(b) Dispersion - Viaduct only H1:H2=6/5

(c) Flow - Viaduct & Barrier H1:H2=6/5

(d) Dispersion - Viaduct & Barrier H1:H2=6/5

(e) Flow - Viaduct only H1:H2=2/1

(f) Dispersion - Viaduct only H1:H2=2/1

(g) Flow - Viaduct & Barrier H1:H2=2/1

(h) Dispersion - Viaduct & Barrier H1:H2=2/1

Flow pattern and dispersion pattern in a step-up street canyon.

When barriers are used (Fig. 8(c)), this vortex is severed into three by the two barriers. This hinders the air exchange between above the viaduct and other areas. In this configuration, pollutants released from viaduct mainly gather at the leeward barrier (Fig. 8(d)). Some particles gather near to the outer walls of the viaduct because of the two weak vortexes.

When the ratio H1/H2 increases to 2 (Fig. 8(e)–(h)), a couple of vortexes with different directions form (Fig. 8 (e)). The upper main vortex locates above the windward building roof and takes more than half of the canyon space. The weak vortex forms at the lower half of the canyon. Fig. 8(f) shows that when H1/H2 = 2, most pollutants are transported to the windward side of the canyon. Furthermore, pollutants do not gather near the viaduct. All these phenomena are caused by the flow. The main clockwise vortex forms above the lower building that in windward side within the canyon. A secondary lower vortex forms in an opposite direction inside the canyon. Pollutants within this weaker counter-clockwise vortex are transported to the windward side of the canyon.

When the noise barriers are used in the H1/H2 = 2 canyon (Fig. 8(g)), the lower vortex takes more space in the canyon. It extends from the leeward side to the windward side of the street. In addition, its center is higher than the noise barrier. A weaker vortex forms at the windward outside the viaduct. More pollutants from the viaduct are taken out of the viaduct canyon by the flow above the viaduct (Fig. 8(h)). Meanwhile, fewer pollutants than Case VO2/1 are taken out of the canyon. Besides, more pollutants are taken to the leeward side although the concentration is still less than at the windward side. That is due to the stronger secondary vortex caused by the barrier structure.

Fig. 9(a) shows the vertical profiles of concentration at the windward wall. The curves for step-down canyons with same H1/H2 ratio are nearly identical. When H1/H2 = 6/5, peak value occurs at about 2.5 m, and concentration below 3 m is higher than that above 3 m. The concentration decreases as the height increases until the height is about 3 m. When H1/H2 = 2, the concentration above 3 m is nearly the same. At the height of below 3 m, the concentration increases rapidly as height decreases and reaches the peak point near to the ground. In addition, the concentration at the ground of Case VB2/1 is higher than Case VO2/1. Fig. 9(b) shows the vertical profile of concentration at the leeward wall. When H1/H2 = 6/5, barriers enhance the peak value of the concentration at about 22 m. When H1/H2 = 2, barriers enhance the concentration at heights above 28 m and below 3 m, while reducing the concentration at heights between 3 m and 28 m. The peak point is at 1.7 m and near the breath zone. The peak value of VO1/2 is much bigger than VB1/2. Fig. 9(c) shows the horizontal profile of concentration at breath line. Concentration decreases from the leeward side to windward side when H1/H2 = 6/5. However, it shows the opposite trend when H1/H2 = 2. Moreover, barriers enhance the concentration at breath line. Comparison of integral concentration between these cases can be seen from Fig. 9 (d). Integral concentrations of all three zones decrease a little when noise barriers are built in the canyon where H1/H2 = 6/5. But integral concentrations of all three zones increase when noise barriers are built in the canyon where H1/H2 = 2. Integral concentration in Zone B is higher than in Zone A when H1/H2 = 2 due to the vortexes. The main clockwise vortex forms above the lower building that in windward side in the canyon. A secondary lower vortex forms in an opposite direction inside the canyon. Pollutants within the weaker counter-clockwise vortex are transported to the windward side of the canyon. This is different from all the other cases.

Fig. 9

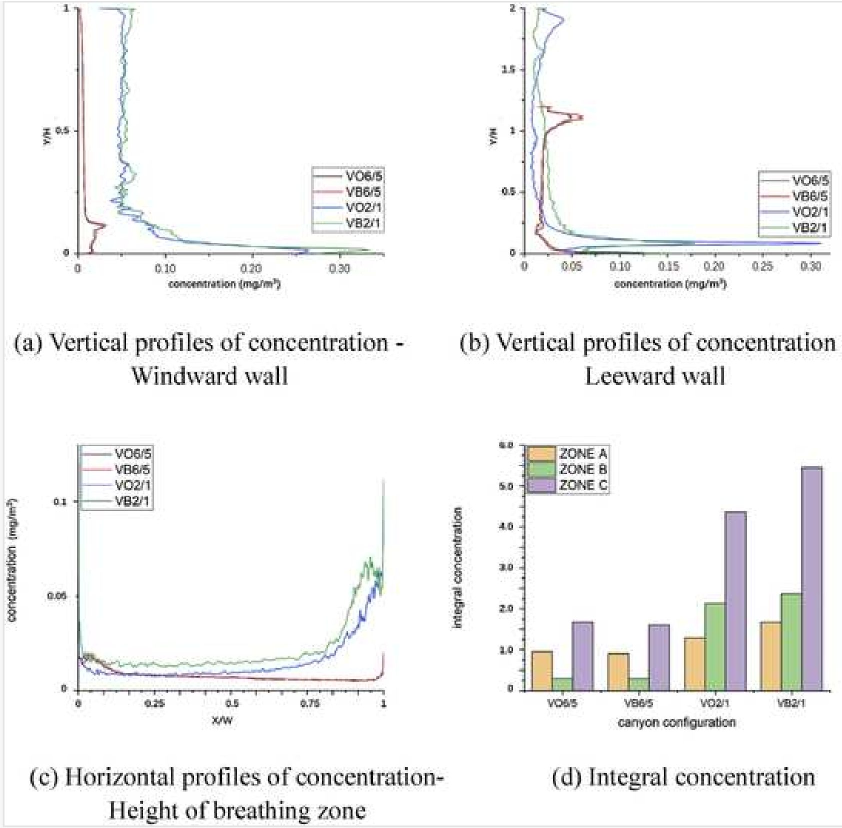

Concentration in a step-down street canyon.

To further analyze the impact of building configuration on the pollutant concentrations in street canyon with viaduct and noise barriers, results of different H1/H2 ratios with viaduct and noise barriers are all listed in Fig. 10. From Case VB1/1 to VB5/6 to VB1/2, it shows a remarkable consistency. As the H1/H2 ratio decrease, the integral concentration in the three zones increases. That is because the higher windward building hinders the pollution spreading out of the street canyon via the airflow. The higher the windward building, the more difficult the diffusion is. Case VB6/5 has the lowest integral concentration among all these cases. The reason is that the top edge of the vortex is higher than the windward building. Therefore, pollutant can be easily transported out of the canyon by airflow from the top of the windward building. In Case VB2/1, integral concentration increases obviously. Although the windward building is lower than the leeward building, pollutant cannot be transported out of the canyon from the top of the windward building. That is because of the stronger upper main vortex located above the windward building roof. As a result, the pollutant is transported to the windward side of the canyon by the weaker lower vortex.

Fig. 10

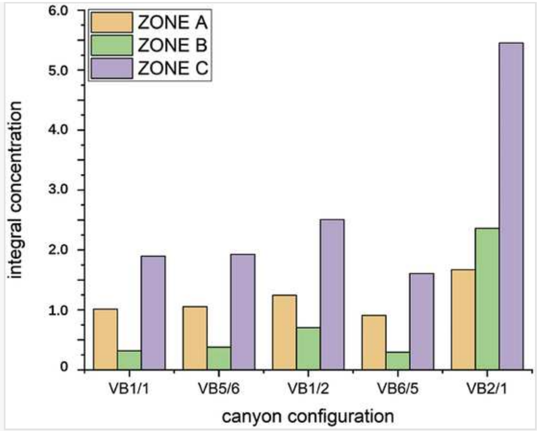

Pollutant dispersion comparison among different H1/H2 ratio.

5 Conclusions and recommendations

5.1 Conclusion

This paper studied inert particulate matter pollutant dispersion in real size urban street canyons combined the effects of the viaduct, noise barriers and asymmetry street canyons on flow regime and pollutant dispersion, using a DPM (discrete phase model) for the commercial software Fluent. Symmetric canyons, step-up canyons and step-down canyons were investigated.

Results show that the height difference between buildings on the two sides of the street is influential to pollutant dispersion. Viaduct introduces more sources of particulate and influences the flow pattern significantly. New vortexes form when noise barriers set up along the viaduct and influence the flow around the viaduct and distribution of pollutants at the center of the canyon but influence to a less extent in the key breathing zones.

When the street canyon is symmetric, barriers can reduce the peak value of pollutant concentration at the windward wall and leeward wall notably. The points where the peak concentrations of the windward wall and leeward wall were located at about 2 m and 19 m, respectively, above the ground. Meanwhile, barriers can lower the integral concentration in zones that affect people's breathing. In conclusion, even though much more pollution is caused by the viaduct, noise barriers on it can help to reduce it to a lower level and reduce viaduct's impact on people's health.

When the street canyon is a step-up type, barriers affect to a less extent the PM distributions at the leeward wall, windward wall, the height of breathing zone and integral concentration of the breathing zones. At the same time, the concentration at all the observed zones when H1/H2 = 1/2 is higher than the concentration with H1/H2 = 5/6. That means in step-up street canyons, the higher the windward building, the more hindered the dispersion of pollutants will be. People live in the windward building or walking on the street have to suffer more from the pollutant.

When the street canyon is a step-down type, the situation is more complex. When H1/H2 = 6/5, pollutants still gather at the leeward wall. The point where the peak concentration at the windward side is found at about 2 m and is about 22 m (about the 6th floor) at the leeward side. Benefiting from the slightly shorter windward building, more pollutants are taken outside the canyon. Thus, it has the least integral pollutant concentration in zone A-C among all the configurations observed in this paper. When H1/H2 = 2, the pollutant is transported to the windward wall and accumulated because of the upper main vortex above the lower building in the canyon. The point of peak concentration is located near the ground at both leeward and windward wall, which means pedestrians' breathing zone is extremely high, and people living on the first floor suffer most.

5.2 Recommendations

It is worth noting that the current numerical simulations are based on a 2D model. As a result, some flow phenomena cannot be shown. Particles can only escape from the top of the canyon, while they can escape from the gaps between buildings on the same side in a 3D model. More over, bridge columns can be embodied in the model which may also have an influence on the pollutant dispersion. In a 3D model, transient wind flow model, flow patterns and pollutant dispersion patterns may differ from the results obtained in this paper. Further studies are recommended to focus on a 3D non-steady model. In a 3D model, bridge columns will be introduced to study the influence of a viaduct more comprehensively. Model will based on a real crossroad with more buildings so that the wind flow and pollutant dispersion are closer to the real conditions.

Street canyons are known for their effect of trapping air pollutants from road vehicles, which pose harmful health effects to people who travel by bicycle or on foot, and people who live or work in the nearby buildings. This paper establishes a method to model the exposures at different street configurations. Other measures are being investigated to reduce the emissions or mitigate their health effects on road users. These measures range from restrictions of vehicle speed and access to the construction of pollutant absorbing pavement.

Acknowledgements

The work described in this paper was financially supported by National Natural Science Foundation of China (No.50808124).

Appendix A Supplementary data

Supplementary data to this article can be found online at https://doi.org/10.1016/j.apr.2019.07.003.

References

The corrections made in this section will be reviewed and approved by journal production editor.

Ai, Z.T., Mak, C.M., 2017. CFD simulation of flow in a long street canyon under a perpendicular wind direction: evaluation of three computational settings. Build. Environ. 114. Available from: https://doi.org/10.1016/j.buildenv.2016.12.032.

Allegrini, J., Dorer, V., Carmeliet, J., 2014. Buoyant flows in street canyons: validation of CFD simulations with wind tunnel measurements. Build. Environ. 72, 63–74. Available from: https://doi.org/10.1016/j.buildenv.2013.10.021.

Allegrini, J., Dorer, V., Carmeliet, J., 2013. Wind tunnel measurements of buoyant flows in street canyons. Build. Environ. 59, 315–326. Available from: https://doi.org/10.1016/j.buildenv.2012.08.029.

Baldauf, R.W., Isakov, V., Deshmukh, P., Venkatram, A., Yang, B., Zhang, K.M., 2016. Influence of solid noise barriers on near-road and on-road air quality. Atmos. Environ. 129, 265–276. Available from: https://doi.org/10.1016/j.atmosenv.2016.01.025.

Beelen, R., Raaschou-Nielsen, O., Stafoggia, M., et al., 2014. Effects of long-term exposure to air pollution on natural-cause mortality: an analysis of 22 European cohorts within the multicentre ESCAPE project. Lancet 383, 785–795. Available from: https://doi.org/10.1016/S0140-6736(13)62158-3.

Beelen, R., Stafoggia, M., Raaschou-Nielsen, O., et al., 2014. Long-term exposure to air pollution and cardiovascular mortality: an analysis of 22 European cohorts. Epidemiology 25, 368–378. Available from: https://doi.org/10.1097/EDE.0000000000000076.

Bowker, G.E., Baldauf, R., Isakov, V., Khlystov, A., Petersen, W., 2007. The effects of roadside structures on the transport and dispersion of ultrafine particles from highways. Atmos. Environ. 41, 8128–8139. Available from: https://doi.org/10.1016/j.atmosenv.2007.06.064.

Carpentieri, M., Kumar, P., Robins, A., 2011. An overview of experimental results and dispersion modelling of nanoparticles in the wake of moving vehicles. Environ. Pollut. 159, 685–693. Available from: https://doi.org/10.1016/j.envpol.2010.11.041.

2018. In: China Vehicle Environmental Management Annual Report (China).

Commission, E., 2008. Commission Regulation (EC) No 692/2008 of 18 July 2008 implementing and amending Regulation (EC) No 715/2007 of the European Parliament and of the Council on type-approval of motor vehicles with respect to emissions from light passenger and commercial veh. Off. J. Eur. Union 199, 1–136.

Fallah-Shorshani, M., Shekarrizfard, M., Hatzopoulou, M., 2017. Integrating a street-canyon model with a regional Gaussian dispersion model for improved characterisation of near-road air pollution. Atmos. Environ. 153, 21–31. Available from: https://doi.org/10.1016/j.atmosenv.2017.01.006.

Fluent, A., 2009. In: 12.0 Theory Guide, vol. 5. Ansys Inc.

Gosman, A.D., loannides, E., 1983. Aspects of computer simulation of liquid-fueled combustors. J. Energy 7, 482–490. Available from: https://doi.org/10.2514/3.62687.

Gu, M., Chen, L., Xiang, H., 1997. Study on the joint probability density function between the wind velocity and direction in Shanghai district. J. Tongji Univ. 25, 166–170.

Habilomatis, G., Chaloulakou, A., 2015. A CFD modeling study in an urban street canyon for ultrafine particles and population exposure: the intake fraction approach. Sci. Total Environ. 530–531, 227–232. Available from: https://doi.org/10.1016/j.scitotenv.2015.03.089.

Hagler, G.S.W., Lin, M., Khlystov, A., Baldauf, R.W., Isakov, V., Faircloth, J., Jackson, L.E., 2012. Science of the Total Environment Field investigation of roadside vegetative and structural barrier impact on near-road ultra fi ne particle concentrations under a variety of wind conditions. Sci. Total Environ. 419, 7–15. Available from: https://doi.org/10.1016/j.scitotenv.2011.12.002.

Hang, J., Lin, M., Wong, D.C., Wang, X., Wang, B., Buccolieri, R., 2016. On the influence of viaduct and ground heating on pollutant dispersion in 2D street canyons and toward single-sided ventilated buildings. Atmos. Pollut. Res. 7, 817–832. Available from: https://doi.org/10.1016/j.apr.2016.04.009.

Hang, J., Luo, Z., Wang, X., He, L., Wang, B., Zhu, W., 2017. The influence of street layouts and viaduct settings on daily carbon monoxide exposure and intake fraction in idealized urban canyons. Environ. Pollut. 220, 72–86. Available from: https://doi.org/10.1016/j.envpol.2016.09.024.

He, L., Hang, J., Wang, X., Lin, B., Li, X., Lan, G., 2017. Numerical investigations of flow and passive pollutant exposure in high-rise deep street canyons with various street aspect ratios and viaduct settings. Sci. Total Environ. 584 (585), 189–206. Available from: https://doi.org/10.1016/j.scitotenv.2017.01.138.

Jin, X., Yang, L., Du, X., Yang, Y., 2016. Sensitivity analyses of ultrafine particle dispersion inside an isolated street canyon. Powder Technol. 304, 143–156. Available from: https://doi.org/10.1016/j.powtec.2016.07.060.

Kastner-Klein, P., Plate, E.J., 1999. Wind-tunnel study of concentration fields in street canyons. Atmos. Environ. 33, 3973–3979. Available from: https://doi.org/10.1016/S1352-2310(99)00139-9.

Kim, J.J., Baik, J.J., 2001. Urban street-canyon flows with bottom heating. Atmos. Environ. 35, 3395–3404. Available from: https://doi.org/10.1016/S1352-2310(01)00135-2.

Kumar, P., Fennell, P., Britter, R., 2008. Measurements of particles in the 5-1000 nm range close to road level in an urban street canyon. Sci. Total Environ. 390, 437–447. Available from: https://doi.org/10.1016/j.scitotenv.2007.10.013.

Kumar, P., Garmory, A., Ketzel, M., Berkowicz, R., Britter, R., 2009. Comparative study of measured and modelled number concentrations of nanoparticles in an urban street canyon. Atmos. Environ. 43, 949–958. Available from: https://doi.org/10.1016/j.atmosenv.2008.10.025.

Kumar, P., Ketzel, M., Vardoulakis, S., Pirjola, L., Britter, R., 2011. Dynamics and dispersion modelling of nanoparticles from road traffic in the urban atmospheric environment-A review. J. Aerosol Sci. 42, 580–603. Available from: https://doi.org/10.1016/j.jaerosci.2011.06.001.

Li, X.L., Wang, J.S., Tu, X.D., Liu, W., Huang, Z., 2007. Vertical variations of particle number concentration and size distribution in a street canyon in Shanghai, China. Sci. Total Environ. 378, 306–

316. Available from: https://doi.org/10.1016/j.scitotenv.2007.02.040.

Li, X.X., Britter, R., Norford, L.K., 2016. Effect of stable stratification on dispersion within urban street canyons: a large-eddy simulation. Atmos. Environ. 144, 47–59. Available from: https://doi.org/10.1016/j.atmosenv.2016.08.069.

Li, X.X., Liu, C.H., Leung, D.Y.C., 2005. Development of a k-e model for the determination of air exchange rates for street canyons. Atmos. Environ. 39, 7285–7296. Available from: https://doi.org/10.1016/j.atmosenv.2005.09.007.

Llaguno-Munitxa, M., Bou-Zeid, E., Hultmark, M., 2017. The influence of building geometry on street canyon air flow: validation of large eddy simulations against wind tunnel experiments. J. Wind Eng. Ind. Aerodyn. 165, 115–130. Available from: https://doi.org/10.1016/j.jweia.2017.03.007.

Madalozzo, D.M.S., Braun, A.L., Awruch, A.M., Morsch, I.B., 2014. Numerical simulation of pollutant dispersion in street canyons: geometric and thermal effects. Appl. Math. Model. 38. Available from: https://doi.org/10.1016/j.apm.2014.04.041.

Meroney, R.N., Pavageau, M., Rafailidis, S., Schatzmann, M., 1996. Study of line source characteristics for 2-D physical modelling of pollutant dispersion in street canyons. J. Wind Eng. Ind. Aerodyn. 62, 37–56. Available from: https://doi.org/10.1016/S0167-6105(96)00057-8.

Moonen, P., Dorer, V., Carmeliet, J., 2011. Evaluation of the ventilation potential of courtyards and urban street canyons using RANS and LES. J. Wind Eng. Ind. Aerodyn. 99, 414–423. Available from: https://doi.org/10.1016/j.jweia.2010.12.012.

Moradpour, M., Afshin, H., Farhanieh, B., 2017. A numerical investigation of reactive air pollutant dispersion in urban street canyons with tree planting. Atmos. Pollut. Res. 8, 253–266. Available from: https://doi.org/10.1016/j.apr.2016.09.002.

Neft, I., Scungio, M., Culver, N., Singh, S., 2016. Simulations of aerosol filtration by vegetation: validation of existing models with available lab data and application to near-roadway scenario. Aerosol Sci. Technol. 50, 937–946. Available from: https://doi.org/10.1080/02786826.2016.1206653.

Ng, W.Y., Chau, C.K., 2014. A modeling investigation of the impact of street and building configurations on personal air pollutant exposure in isolated deep urban canyons. Sci. Total Environ. 468–469, 429–448. Available from: https://doi.org/10.1016/j.scitotenv.2013.08.077.

Nikolova, I., Janssen, S., Vos, P., Vrancken, K., Mishra, V., Berghmans, P., 2011. Dispersion modelling of traffic induced ultrafine particles in a street canyon in Antwerp, Belgium and comparison with observations. Sci. Total Environ. 412–413, 336–343. Available from: https://doi.org/10.1016/j.scitotenv.2011.09.081.

Oke, T.R., 1988. Street design and urban canopy layer climate. Energy Build. 11, 103–113. Available from: https://doi.org/10.1016/0378-7788(88)90026-6.

Quang, T.N., He, C., Morawska, L., Knibbs, L.D., Falk, M., 2012. Vertical particle concentration profiles around urban office buildings. Atmos. Chem. Phys. 12, 5017–5030. Available from: https://doi.org/10.5194/acp-12-5017-2012.

Santiago, J.L., Martín, F., 2008. SLP-2D: a new Lagrangian particle model to simulate pollutant dispersion in street canyons. Atmos. Environ. 42, 3927–3936. Available from: https://doi.org/10.1016/j.atmosenv.2007.05.038.

Scungio, M., Stabile, L., Rizza, V., Pacitto, A., Russi, A., Buonanno, G., 2018. Science of the Total Environment Lung cancer risk assessment due to traf fi c-generated particles exposure in urban street canyons: a numerical modelling approach. Sci. Total Environ. 631–632, 1109–1116. Available from: https://doi.org/10.1016/j.scitotenv.2018.03.093.

Shanghai Government, 2018. In: Shanghai Master Plan (2017-2035), Shanghai Government, pp. 57–60. Available from: http://www.shanghai.gov.cn/newshanghai/xxgkfj/2035002.pdf.

Sini, J.F., Anquetin, S., Mestayer, P.G., 1996. Pollutant dispersion and thermal effects in urban street canyons. Atmos. Environ. 30, 2659–2677. Available from: https://doi.org/10.1016/1352-2310(95)00321-5.

Steffens, J.T., Wang, Y.J., Zhang, K.M., 2012. Exploration of effects of a vegetation barrier on particle size distributions in a near-road environment. Atmos. Environ. 50, 120–128. Available from: https://doi.org/10.1016/j.atmosenv.2011.12.051.

Tan, Z., Dong, J., Xiao, Y., Tu, J., 2015. A numerical study of diurnally varying surface temperature on flow patterns and pollutant dispersion in street canyons. Atmos. Environ. 104. Available from: https://doi.org/10.1016/j.atmosenv.2015.01.027.

Venkatram, A., Isakov, V., Deshmukh, P., Baldauf, R., 2016. Modeling the impact of solid noise barriers on near road air quality. Atmos. Environ. 141, 462–469. Available from: https://doi.org/10.1016/j.atmosenv.2016.07.005.

Wang, L., Pan, Q., Zheng, X.P., Yang, S.S., 2017. Effects of low boundary walls under dynamic inflow on flow field and pollutant dispersion in an idealized street canyon. Atmos. Pollut. Res. 8, 564–575. Available from: https://doi.org/10.1016/j.apr.2016.12.004.

Wang, M., Beelen, R., Stafoggia, M., et al., 2014. Long-term exposure to elemental constituents of particulate matter and cardiovascular mortality in 19 European cohorts: results from the ESCAPE and transphorm projects. Environ. Int. 66, 97–106. Available from: https://doi.org/10.1016/j.envint.2014.01.026.

Wania, A., Bruse, M., Blond, N., Weber, C., 2012. Analysing the influence of different street vegetation on traffic-induced particle dispersion using microscale simulations. J. Environ. Manag. 94, 91–101. Available from: https://doi.org/10.1016/j.jenvman.2011.06.036.

Xia, J., Leung, D.Y.C., 2001. A concentration correction scheme for Lagrangian particle model and its application in street canyon air dispersion modelling. Atmos. Environ. 35, 5779–5788. Available from: https://doi.org/10.1016/S1352-2310(01)00358-2.

Xiaomin, X., Zhen, H., Jiasong, W., 2006. The impact of urban street layout on local atmospheric environment. Build. Environ. 41, 1352–1363. Available from: https://doi.org/10.1016/j.buildenv.2005.05.028.

Xie, X., Liu, C.H., Leung, D.Y.C., 2007. Impact of building facades and ground heating on wind flow and pollutant transport in street canyons. Atmos. Environ. 41, 9030–9049. Available from: https://doi.org/10.1016/j.atmosenv.2007.08.027.

Xie, X., Liu, C.H., Leung, D.Y.C., Leung, M.K.H., 2006. Characteristics of air exchange in a street canyon with ground heating. Atmos. Environ. 40, 6396–6409. Available from: https://doi.org/10.1016/j.atmosenv.2006.05.050.

Yoshie, R., Mochida, A., Tominaga, Y., Kataoka, H., Harimoto, K., Nozu, T., Shirasawa, T., 2007. Cooperative project for CFD prediction of pedestrian wind environment in the architectural institute of Japan. J. Wind Eng. Ind. Aerodyn. 95, 1551–1578. Available from: https://doi.org/10.1016/j.jweia.2007.02.023.

Zhong, J., Cai, X.M., Bloss, W.J., 2017. Large eddy simulation of reactive pollutants in a deep urban street canyon: coupling dynamics with O3-NOx-VOC chemistry. Environ. Pollut. 224, 171–184. Available from: https://doi.org/10.1016/j.envpol.2017.01.076.

Footnotes

Article Footnotes

Peer review under responsibility of Turkish National Committee for Air Pollution Research and Control.

Graphical abstract

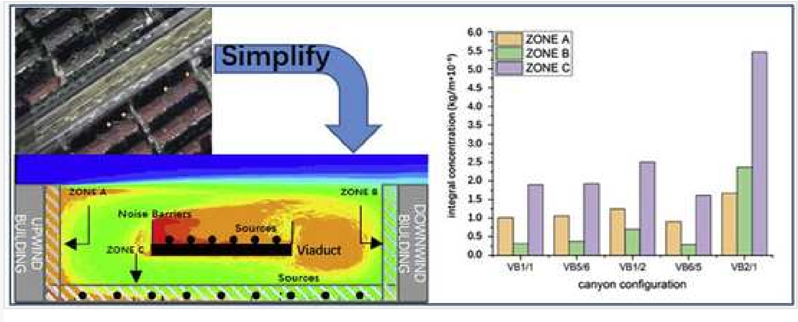

Highlights

- ~~The influence of viaduct, noise barrier, and the building configuration on particulate matters (PM) dispersion in street canyon was study.~~The influence of viaduct, noise barrier, and the building configuration on PM dispersion in street canyon was study.
- Viaduct can keep more pollutants within the street canyon and influence the flow pattern significantly.
- ~~Noise barriers mainly influence the flow and distribution of pollutants at the center of the canyon but influence to a less extent in the key breathing zones.~~Noise barriers mainly influence the pollutant distribution at the center of the canyon but less in the key breathing zones.
- A higher downwind building than the upwind building can hinder the diffusion of pollutants.

Appendix A Supplementary data

The following is the Supplementary data to this article:

Multimedia Component 1

Multimedia component 1

Queries and Answers

Query: Your article is registered as a regular item and is being processed for inclusion in a regular issue of the journal. If this is NOT correct and your article belongs to a Special Issue/Collection please contact m.anthony.1@elsevier.com immediately prior to returning your corrections.

Answer: Yes

Query: Please confirm that the provided email “xiexiaomin@sjtu.edu.cn” is the correct address for official communication, else provide an alternate e-mail address to replace the existing one, because private e-mail addresses should not be used in articles as the address for communication.

Answer: This is excatly the correct address for offical communication. Thank you for reminding.

Query: Please confirm that given names and surnames have been identified correctly and are presented in the desired order and please carefully verify the spelling of all authors' names.

Answer: Yes

Query: The citation ‘Hagler and Kumar et al. (2012)’ has been changed to match the name in the reference list. Please check here and in subsequent occurrences, and correct if necessary.

Answer: I have revised the cites, but it seems in wrong citation format. Could you please help me to fix this? Thank you very much. "Kumar et al. " and the closing parenthese after "2012"are not linked as citation.

Query: Ref. “Shanghai Government, 2018” is cited in the text but not provided in the reference list. Please provide it in the reference list or delete these citations from the text.

Answer: The reference has been added, but I cannot link the citation because "Due to technical issue, Proof Central could not execute the change. Please execute it in XML." So it is now listed as uncited reference. Could you please help me with that?

Query: Have we correctly interpreted the following funding source(s) and country names you cited in your article: National Natural Science Foundation of China, China?

Answer: Yes

Query: Highlights should only consist of “125” characters per bullet point, including spaces. The highlights provided are too long; please edit them to meet the requirement.

Answer: The hightlight has been edited to meet the requirement.